

Fig. 12. Transit time versus length for aluminum rods.

the first received signal influences the accuracy of the  $\Delta T$  measurement. More accurate measurements can be made when the first-arrival signal has a fast rise time. An electronic counter-timer is not useful in this method because the rise times obtained with and without a sample are frequently different. However, the calibrated variable time delay line in the oscilloscope can be used to measure  $\Delta T$  with a visual resolution of about  $0.1 \mu\text{s}$ .

#### EXPERIMENTAL RESULTS

Examples of experimental results are given for aluminum and for two types of sedimentary rocks. Samples were cut into right cylinders with diameters of 5.08 cm and lengths varying from 1.27 to 10.16 cm. The ends were ground flat with a magnetic-bed reciprocating grinder and were parallel to within 0.025 mm. Samples were prepared from Solenhofen limestone, which is a hard, fine-grained sedimentary rock with a porosity of 2.7 percent and a dry bulk density of  $2.6 \times 10^3 \text{ kg/m}^3$ . Heard [28] states that Solenhofen limestone is mechanically almost isotropic. Boise sandstone is a relatively coarse-grained, well-consolidated rock with a porosity of 26.3 percent and a dry bulk density of  $1.9 \times 10^3 \text{ kg/m}^3$ . Wave velocity studies of King [6] indicate that Boise sandstone is isotropic within the limits of experimental error. Using isotropic materials greatly simplifies the determination of dynamic elastic coefficients because  $P$ -wave and  $S$ -wave velocities need not be measured in more than one direction through the media.

Transit times of  $P$  waves and  $S$  waves are shown in Fig. 12 for seven aluminum rods ranging in length from 1.27 to 10.16 cm. Standard deviations of velocities computed from these data are 13 m/s and 19 m/s for  $P$  waves and  $S$  waves, respectively. Lines drawn through the data points have no intercept when extrapolated to zero length. Hence, electrical delays and phase shifts in the apparatus have negligible effects on measurements.

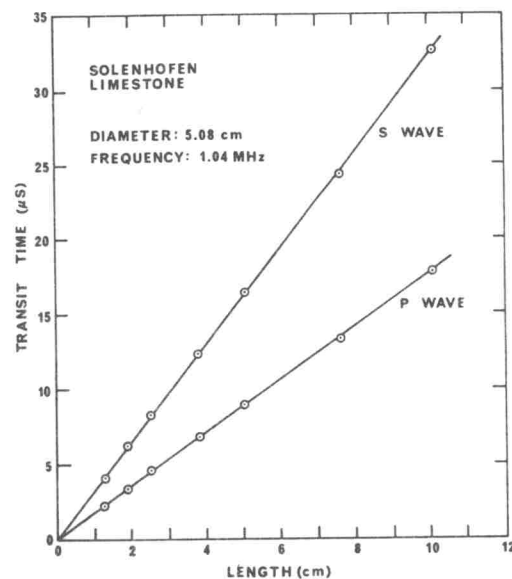


Fig. 13. Transit time versus length for dry Solenhofen limestone samples under uniform pressure of  $20.7 \times 10^6 \text{ N/m}^2$ .

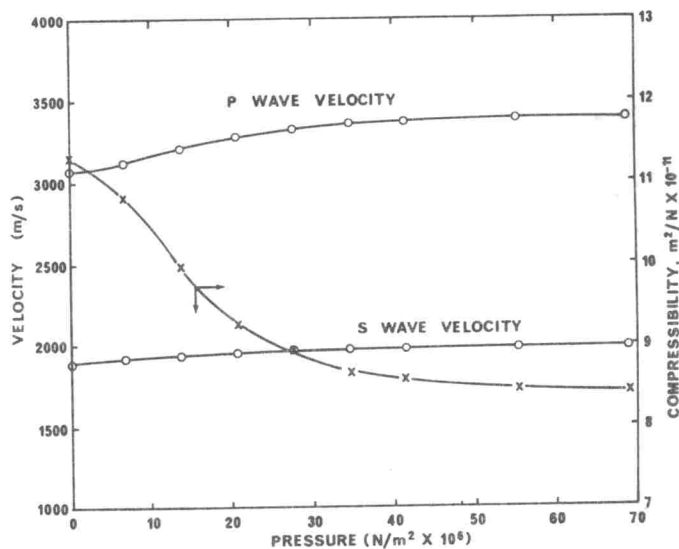


Fig. 14. Velocity and bulk compressibility as a function of uniform pressure for dry Boise sandstone.

Similar plots in Fig. 13 show that reasonably linear relations between transit time and length are also obtained for dry samples of Solenhofen limestone. These samples were tested under uniform pressures of  $3000 \text{ lbf/in}^2$  ( $20.7 \times 10^6 \text{ N/m}^2$ ). Standard deviations were 62 m/s and 39 m/s, respectively, for  $P$ -wave and  $S$ -wave velocities. Differences in homogeneity of individual samples, as well as experimental errors, influence the variance in the velocity of rocks.

Results of velocity measurements on dry Boise sandstone under uniform external pressure are shown in Fig. 14. Both  $P$ -wave and  $S$ -wave velocities increase as microcracks are closed by the application of pressure. Since Boise sandstone is isotropic, the elastic moduli (Table II) were computed from well-known relations for isotropic bodies (see the Appendix). Increased pressure on the rock

TABLE II  
VELOCITIES AND DYNAMIC ELASTIC MODULI FOR DRY BOISE SANDSTONE UNDER UNIFORM PRESSURE

| Uniform Pressure<br>(N/m <sup>2</sup> × 10 <sup>6</sup> ) | Velocity        |                 | Poisson's Ratio | Bulk Modulus<br>(N/m <sup>2</sup> × 10 <sup>11</sup> ) | Rigidity Modulus<br>(N/m <sup>2</sup> × 10 <sup>11</sup> ) | Young's Modulus<br>(N/m <sup>2</sup> × 10 <sup>11</sup> ) | Bulk Compressibility<br>(m <sup>2</sup> /N × 10 <sup>-11</sup> ) |
|-----------------------------------------------------------|-----------------|-----------------|-----------------|--------------------------------------------------------|------------------------------------------------------------|-----------------------------------------------------------|------------------------------------------------------------------|
|                                                           | P Wave<br>(m/s) | S Wave<br>(m/s) |                 |                                                        |                                                            |                                                           |                                                                  |
| 0                                                         | 3069            | 1890            | 0.195           | 0.088                                                  | 0.068                                                      | 0.162                                                     | 11.30                                                            |
| 6.89                                                      | 3124            | 1914            | 0.200           | 0.093                                                  | 0.070                                                      | 0.167                                                     | 10.80                                                            |
| 13.79                                                     | 3206            | 1935            | 0.214           | 0.100                                                  | 0.071                                                      | 0.173                                                     | 9.96                                                             |
| 20.68                                                     | 3280            | 1951            | 0.226           | 0.108                                                  | 0.072                                                      | 0.177                                                     | 9.26                                                             |
| 27.58                                                     | 3322            | 1966            | 0.231           | 0.112                                                  | 0.073                                                      | 0.181                                                     | 8.95                                                             |
| 34.47                                                     | 3353            | 1969            | 0.237           | 0.115                                                  | 0.074                                                      | 0.182                                                     | 8.67                                                             |
| 41.37                                                     | 3362            | 1972            | 0.238           | 0.116                                                  | 0.074                                                      | 0.183                                                     | 8.60                                                             |
| 55.16                                                     | 3380            | 1978            | 0.240           | 0.118                                                  | 0.074                                                      | 0.184                                                     | 8.48                                                             |
| 68.95                                                     | 3391            | 1984            | 0.240           | 0.119                                                  | 0.075                                                      | 0.185                                                     | 8.42                                                             |

causes the elastic moduli to increase and the compressibility to decrease as expected. Uniform pressures on Boise sandstone were limited to 10 000 lbf/in<sup>2</sup> ( $68.9 \times 10^6$  N/m<sup>2</sup>) in order to prevent any damage to the porous structure.

#### DISCUSSION

Methods previously developed for simultaneous or consecutive determinations of *P*-wave and *S*-wave velocities of rock samples have used pulses that are essentially square waves and contain a wide spectrum of frequencies. Transit times are determined by locating the onset of first arrivals. These arrivals may have fast- or slow-rise times depending on the shape of the input pulse and the filtering action of the rock. When the rise time is slow, the onset of the signal becomes ambiguous. As a result, the errors in velocity may vary from 1 to 5 percent depending on the rise time. These difficulties are magnified for *S* waves because many *S*-wave sources also generate *P* waves that interfere to a disturbing degree. Previous efforts to avoid interference between modes appear to be based on trial and error methods and are not completely effective.

The dual-mode acoustic apparatus and experimental technique avoid these difficulties and represent a firm improvement over methods currently available for consecutively measuring *P*-wave and *S*-wave velocities in many types of rock. The mechanical design is based upon sound principles of geometrical acoustics. As a result, the relative amounts of acoustic energy transmitted or reflected from various parts of the transducer can be precisely calculated to evaluate the efficiency of the system. The mode-conversion technique for obtaining shear waves has been tested thoroughly in an apparatus described and used previously by the writers [7], [8]. The *P*-wave signals are strong and no mechanical or acoustic interference occurs between modes. The sinusoidal carrier frequency of the tone-burst pulses can be varied from 0.25 to 5 MHz. For work that requires evaluation of acoustic response as a function of frequency, the narrow bandwidth obtained with tone-burst pulses is a definite advantage. Travel-time measurements are made by selecting certain identifiable reference points of the trigger and received sinusoidal pulses as reference

signals that start and stop the counter-timer. For each measurement the reference stop signal is adjusted for constant vertical deflection.

Accuracy of the measurement is determined by the resolution of the counter-timer (0.01  $\mu$ s). The reproducibility is  $\pm 0.01 \mu$ s for a given measurement. Allowing for possible errors in calibration and measurements of sample length, the total errors in the system are less than 1 percent for standard lengths of 3.81 cm. To obtain this degree of accuracy the sample must not cause distortion of the received pulse. A change in pulse shape or carrier frequency may indicate dispersion caused by inhomogeneities in the sample and the validity of results would be in doubt. The nature of nonhomogeneous rocks is so diverse that no universal techniques have been devised that eliminate all possible difficulties. Using V-shaped excitation pulses can extend the capability of the dual-mode apparatus for troublesome materials. However, a certain reduction in resolution must be expected.

The velocities measured with the dual-mode apparatus on samples of aluminum, Solenhofen limestone, and Boise sandstone (Figs. 12-14), agree well with the values published by Peselnick [29], King [6], Gregory [7] and Podio *et al.* [8].

#### SUMMARY

1) An ultrasonic laboratory apparatus and pulse transit-time measurement technique have been developed for determining *P*-wave and *S*-wave velocities of porous solid samples under triaxial pressures up to 25 000 psi ( $172 \times 10^6$  N/m<sup>2</sup>). The apparatus and experimental technique have substantial advantages over existing methods.

2) Transit times of tone-burst pulses through non-dispersive rocks can be determined with a resolution of  $10^{-8}$  second.

3) The new method avoids hysteresis effects encountered in making separate measurements of *P*-wave and *S*-wave velocities and reduces the testing time by one half.

4) An automated data-acquisition system samples and digitizes pulse waveforms and stores the data in a form suitable for analysis by a computer. The same